

NiO Nanoparticles Based Carbon Paste as a Sensor for Detection of Dopamine

Sathish Reddy^{1,2,*}, B.E. Kumara Swamy², Seeram Ramakrishana^{1,5}, Liumin He⁴ and H. Jayadevappa³

¹ Guangdong-Hongkong-Macau Institute of CNS Regeneration (GHMICR), Jinan University, Guangzhou, Guangdong, 510632, China.

² Department of P.G. Studies and Research in Industrial Chemistry, Kuvempu University, Jnana Sahyadri, Shankaraghatta, Shimoga, Karnataka 577451, India.

³ Department of Chemistry, Sahyadri Science College, Shimoga, Karnataka, India.

⁴ Department of Biomedical Engineering, College of Life Science and Technology, Jinan University, Guangzhou, Guangdong, 510632, China.

⁵ Center for Nanofibers and Nanotechnology, Department of Mechanical Engineering, Faculty of Engineering, National University of Singapore, Singapore, 117576.

*E-mail: sathish-cnc@pku.edu.cn, & gnsathishreddy@gmail.com

Received: 30 November 2017 / Accepted: 26 January 2018 / Published: 10 May 2018

In this paper, NiO nanoparticles were synthesized using cetyl trimethyl ammonium bromide (CTAB) and sodium dodecyl sulfate (SDS). The prepared NiO nanoparticles were applied for the preparation of modified carbon-paste electrodes (MCPE) for the electrochemical investigations of potassium ferrocyanide $K_4[Fe(CN)_6]$ and dopamine (DA). The MCPE prepared from CTAB-NiO nanoparticles demonstrated an enhanced sensing response for $K_4[Fe(CN)_6]$ and DA as compared with those of the MCPE fabricated from SDS-NiO nanoparticles. The MCPE prepared from SDS/polyglycine/CTAB-NiO nanoparticles demonstrated a further enhanced peak current response and effectively analyzed simultaneously DA, Ascorbic acid (AA), Uric acid (UA) and Bisphenol-A (BPA).

Keywords: NiO nanoparticles, Dopamine, Carbon Paste Electrode, Cyclic Voltammetry and Differential pulse voltammetry.

1. INTRODUCTION

Nickel (II) oxide nanoparticle is a p-type semiconductor metal oxide having a constant wide band gap. In addition, it can be useful as a transparent p-type semiconductor layer [1]. Ultra-fine NiO nano-ceramic particles with a homogeneous size and well distribution characteristics are powerfully

attractive for various applications, examples; Synthesis of sensors, magnetic materials, electrochromic, composite, heterogeneous catalytic materials, etc [2]. Recently, the NiO nanoparticles has been used for preparation of modified electrode for electrochemical detection of numerous important compounds such as; gases [3], hydrogen peroxide [4], cytochrome c [5], desmopressin and L-glutathione [6], DNA [7], CO and NO₂ gases [2], glucose [8], insulin [9], hemoglobin [10], hydrazine [11], toluene [12] and uric acid [13].

Dopamine (DA) is a significant catecholamine neurotransmitter in the brain. Degeneration of dopaminergic neurons is the most important cause of Parkinson's disease (PD), with which more or less 500,000 people in the United States have been analyzed [14], and causes reduce in concentration of DA, still DA decreases, in the striatum and probably in other basal ganglia areas [15,16]. DA is electrochemically active (oxidizable and reducible), which permits electrochemical methods to be working for the detection of DA concentrations. Electrochemical detection is a very easy, eco-friendly and sensitive detection method for the investigation of colored or turbid samples. However, the electrochemical method detection of DA in physiological samples is exciting research because of the high concentrations of ascorbic acid (AA) that together with the low concentrations of DA in physiological body fluid samples [15-21]. Uric acid (UA) is the key in end product of purine metabolism. Uneven concentrations of UA are symptoms of a number of diseases for instance gout, Lesch-Nyan disease and hyperuricemia [22]. Furthermore, almost all of bare electrodes, DA, UA and AA attain oxidized at roughly the same potential value, resultant in overlapped voltammetric response. Simultaneous detection of DA, UA and AA is a complexity of serious significance not only in the field of neurochemistry and biomedical chemistry but also for pathological and diagnostic research. At the same time Bisphenol-A [2, 2-bis (4-hydroxyphenyl) propane, BPA] is generally used in the plastic industry as a monomer. In modern studies with rodent's exhibit that BPA elicits a huge range of activities, as well as neurochemical alterations [23, 24]. Interestingly, simultaneous detection of DA, AA, UA and BPA in physiological phosphate buffer solutions places very significant role in the research field.

In the present work, SDS- NiO nanoparticles and CTAB- NiO nanoparticles were synthesized by a co-precipitation method based on a changed version of the method reported in the literature [25, 26]. The prepared NiO nanoparticles were characterized by SEM, UV-vis spectroscopy, XRD and TEM. The obtained NiO nanoparticles were used for the preparation of a modified carbon-paste electrode (MCPE) for the electrochemical detection of dopamine in the pH range from 5.5 to 8.0 PBS. The MCPE demonstrated an enhanced redox peak current at pH 7.4 PBS. The MCPE prepared with CTAB- NiO nanoparticles demonstrated enhanced peak current response as compared with those of the MCPE prepared with SDS- NiO nanoparticles. The MCPE prepared with CTAB- NiO nanoparticles exhibited a linearly increase in anodic peak current with an increased concentration of DA and detection limit was found to be 6.86×10^{-7} M. The MCPE prepared with SDS/Poly(glycine)/CTAB- NiO nanoparticles was used for electrochemical detection of DA, AA, UA, BPA, and successfully simultaneously detection of DA, AA, UA and BPA at physiological pH 7.4 PBS.

2. EXPERIMENTAL METHODS

2.1. Apparatus

The NiO nanoparticles were characterized by a variety of techniques. UV-visible spectra were obtained on a Perkin Elmer UV-VIS spectrophotometer by dispersing and sonicating NiO nanoparticles in water from a Millipore purification system. Powder XRD patterns were recorded on a Philips XRD X'Pert Pro diffractometer equipped with a Cu-K α radiation ($\lambda=1.5438 \text{ \AA}$) source. The structural morphology of the NiO nanoparticles was studied using a JEOL JSM-848 scanning electron microscope and a JEOL 2000 Fx-II transmission electron microscope equipped with ultra-thin windows from Oxford Instruments. All of the electrochemical experiments were performed using a single-compartment, three-electrode cell with MCPes prepared with SDS-NiO nanoparticles and CTAB- NiO nanoparticles, SDS/polyglycine/CTAB-NiO nanoparticles as the working electrode. An aqueous saturated calomel electrode (SCE) was used as the reference electrode and a Pt wire served as the auxiliary electrode. All potentials were measured and reported vs. the SCE. The cyclic voltammetry (CV) measurements and differential pulse voltammetry (DPV) techniques were performed on a model 660c (CH Instruments) potentiostat/galvanostat.

2.2. Materials

Nickel sulphate (NiSO₄) was purchased from sd. Fine Chemicals. Absolute ethanol (99.9%), sodium hydroxide (NaOH) and graphite powder were from Merck Chemicals and DA, AA, UA, BPA, CTAB and SDS were purchased from Himedia Chemicals. DA stock solution was prepared in 0.1 M perchloric acid, UA stock solution in 0.1 M NaOH, BPA stock solutions was prepared by first dissolved in absolute ethanol then diluted with distilled water. Phosphate buffer solution (PBS) was prepared and the pH can be adjusted by the addition of 0.2 M NaH₂PO₄ and Na₂HPO₄ solutions. All the aqueous solutions were prepared with double-distilled water.

2.3. Preparation of NiO nanoparticles

The SDS-NiO nanoparticles were synthesized according to the co-precipitation method described elsewhere [25, 26] with slight alteration. In a typical experiment, the first solution contained 0.06M NiSO₄.6H₂O, 0.12M acetic acid, 40 mg of SDS and the second solution contained 0.18M NaOH pellets, 100 ml absolute ethanol; all aqueous solutions were prepared by using distilled water, the first solution was added to second solution with continues stirring. The resulting precipitate was filtered by using whatmann filter paper (grade-41) and dried at 80⁰C in hot air oven about 1hour. The dried precipitate was transferred to silica crucible and ignited at 400⁰C for roughly 3 hours. Then obtained powder was washed with ethanol three or four times to remove impurities present in the NiO nanoparticles. The same procedure was followed for the preparation of CTAB-NiO nanoparticles using CTAB as the surfactant. The NiO nanoparticles prepared using SDS was noted as SDS-NiO nanoparticles, as well as CTAB-NiO nanoparticles that were prepared using CTAB.

2.4. Preparation of bare carbon-paste electrode and modified carbon-paste electrode

The bare carbon-paste electrode (bare CPE) was prepared by hand mixing 80% graphite powder with 20% silicon oil in an agate mortar for roughly 30 min to produce a homogenous carbon paste. The paste was packed into the homemade cavity and smoothed on a piece of weighing paper. The modified carbon-paste electrode (MCPE) was prepared by the addition of 10 mg of NiO nanoparticles to the previously prepared graphite powder/silicon oil mixture.

2.5. Preparation of SDS/polyglycine/CTAB- NiO nanoparticle modified carbon paste electrode

The MCPE with SDS/polyglycine/ CTAB- NiO nanoparticle was synthesized by electrochemical polymerization of glycine on the MCPE prepared from CTAB- NiO nanoparticle. The electrochemical polymerization of glycine on the MCPE prepared from CTAB- NiO nanoparticle was performed using a cyclic voltammetric method in an aqueous solution that contained 0.04 M glycine in 0.2 M acetate buffer solution at pH 5.0. Electropolymerization process was achieved by the creation of a film that grew between -0.5 V and 1.8 V at a scan rate of 100 mV/s for five cycles using Cyclic Voltammetry (CV). After polymerization, the electrode was thoroughly washed with distilled water and SDS solution (10 μ L) was added to the surface of the MCPE prepared from polyglycine/ CTAB- NiO nanoparticle nanoparticles for 5 min. The electrode was later carefully rinsed with water to remove unabsorbed modifier and dried in air at room temperature.

3. RESULTS AND DISCUSSION

3.1. Characterization

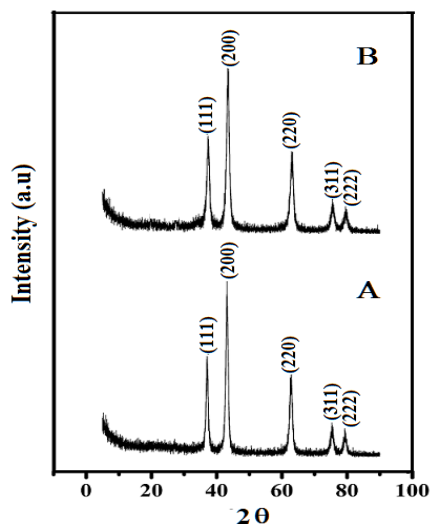


Figure 1. XRD patterns for (A) SDS-NiO nanoparticles and (B) CTAB-NiO nanoparticles.

The XRD pattern of the SDS-NiO nanoparticles and (B) CTAB-NiO nanoparticles are shown in Fig. 1 (A, and (B,). All peaks in Fig.1 can be fit indexed to the face center cubic structure of nickel oxide (JCPDS PDF, no. 780429) with high crystallinity. No impurity peaks of other nickel oxides were observed, which indicates the high purity of the products. The crystallite sizes of the NiO nanoparticles

were calculated using the Debye–Scherrer formula. The obtained average crystalline sizes are 15 and 11 nm for SDS-NiO nanoparticles and CTAB-NiO nanoparticles respectively.

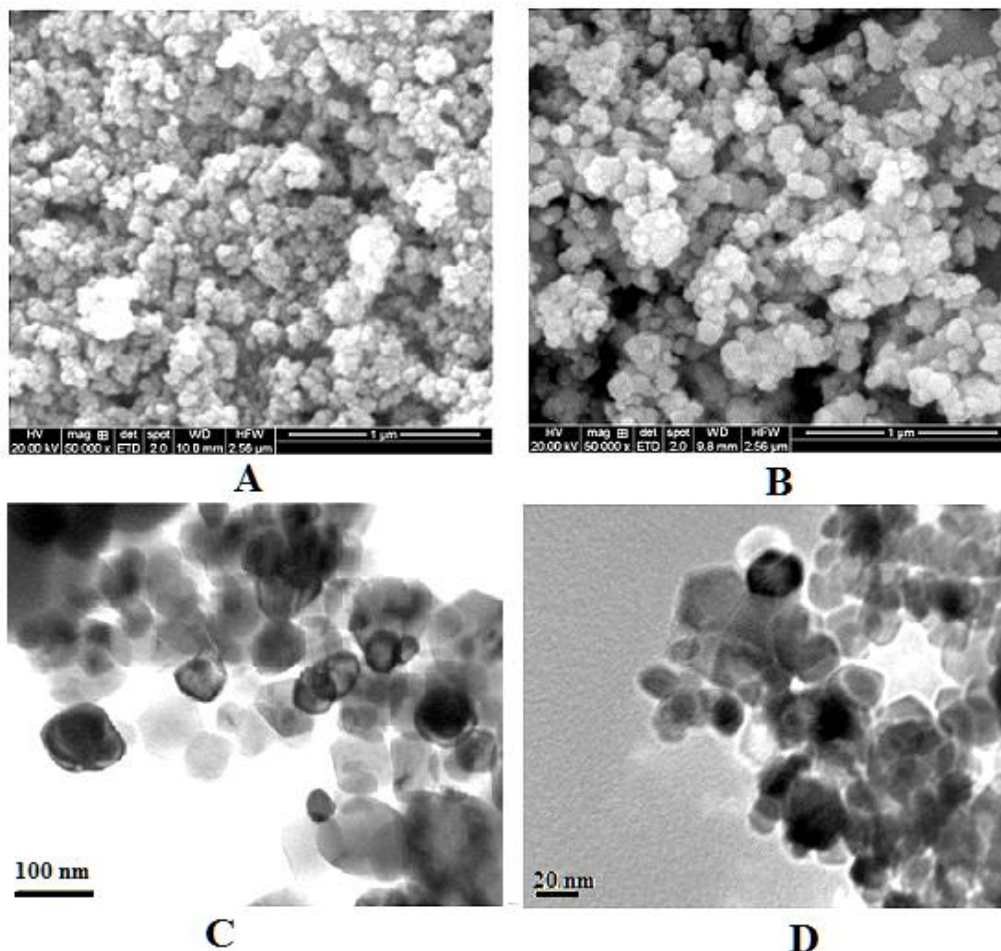


Figure 2. SEM images of (A) SDS-NiO nanoparticles and (B) CTAB-NiO nanoparticles and corresponding TEM images (C) SDS-NiO nanoparticles and (D) CTAB-NiO nanoparticles.

The surface morphology of the SDS-NiO nanoparticles and CTAB-NiO nanoparticles samples was examined using SEM and TEM; the images are shown in Fig. 2 (A)-(D). The SEM and TEM images show different morphologies and sizes for NiO nanoparticles prepared in SDS and CTAB surfactants. An irregular-like morphology was observed for SDS -NiO nanoparticles in the SEM image in Fig. 2 (A) and in the matching TEM image for the same sample in Fig. 2 (C). Upon close very test, the particles in the TEM image were observed to be irregular-shaped with a width of roughly 90 nm. Irregular flake-like morphology was observed for the CTAB-NiO nanoparticles in the SEM image in Fig. 2 (B) and in the matching TEM image for the same sample in Fig. 2 (D). The particles, upon very close test in the TEM image, we observed to be round and flake- irregular shaped with a size of roughly 20 nm.

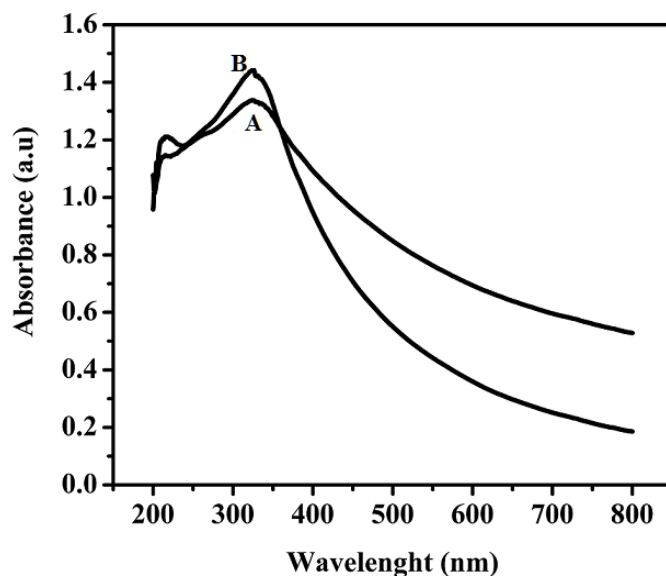


Figure 3. UV-Visible absorption spectra of (A) SDS-NiO nanoparticles and (B) CTAB-NiO nanoparticles samples.

The UV–visible absorption spectra of the NiO nanoparticles dispersed in ethanol solution demonstrate broad absorption peaks centered at roughly 324 nm for the CTAB- NiO nanoparticles and at 325nm for the SDS- NiO nanoparticles, as shown in Fig. 3 (A) and (B).

3.2. Electrochemical response of $K_4 [Fe(CN)_6]$ at bare CPE and MCPEs

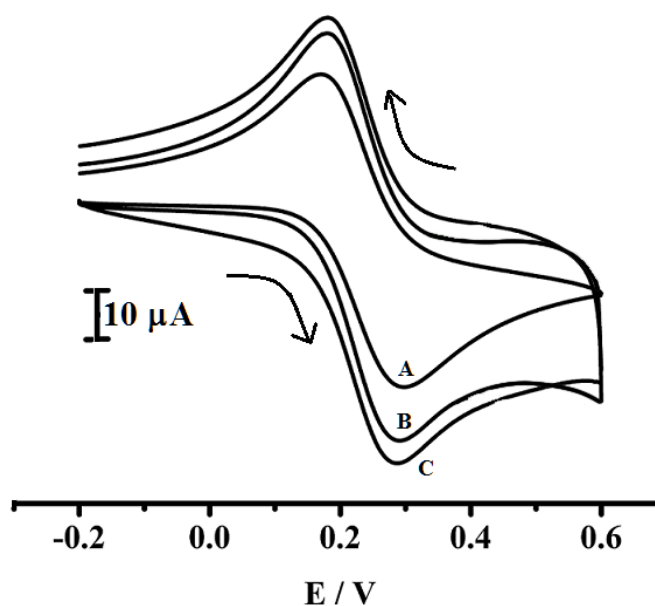


Figure 4. Cyclic voltammogram of 1×10^{-3} M $K_4[Fe(CN)_6]$ in 1M KCl (A) bare CPE, (B) a MCPE prepared with SDS-NiO nanoparticles and (C) a MCPE prepared with CTAB-NiO nanoparticles.

Potassium ferrocyanide was chosen to estimate the performance of the prepared electrode. Fig.4 shows the electrochemical redox peak current response of 1×10^{-3} M $K_4[Fe(CN)_6]$ in 1M KCl at MCPE prepared with SDS-NiO nanoparticles and CTAB-NiO nanoparticles. Due to the complex properties and the irregularity of the electrode surface, the cyclic voltammograms of $K_4[Fe(CN)_6]$ at bare carbon paste electrode (bare CPE) curve (A) is low redox peak current signal. However, the cyclic voltammetric response is apparently enhanced at MCPE prepared from SDS-NiO nanoparticles and CTAB-NiO nanoparticles, reflected by the improvement of the redox peak currents (i_p) and the decline of the electrochemical peaks potential difference curve (B) and (C). The CTAB-NiO nanoparticles MCPE exhibits enhanced redox peak current response with slight reduction of over potential than the SDS-NiO nanoparticles MCPE. This demonstrated that the MCPEs prepared from CTAB-NiO nanoparticles exhibit better electrochemical sensing and electrocatalytic activity.

3.3. Effect of pH

The effect of pH on the detection of 1×10^{-5} M DA in PBS at MCPE prepared with SDS-NiO nanoparticles and CTAB-NiO nanoparticles was analyzed in the pH range of 5.5–8.0 PBS. Graphs of i_{pa} (A) versus the pH of the solution for Bare CPE, MCPEs prepared with SDS-NiO nanoparticles and CTAB-NiO nanoparticles are shown in Fig. 5, (■), (▲) and (●) respectively.

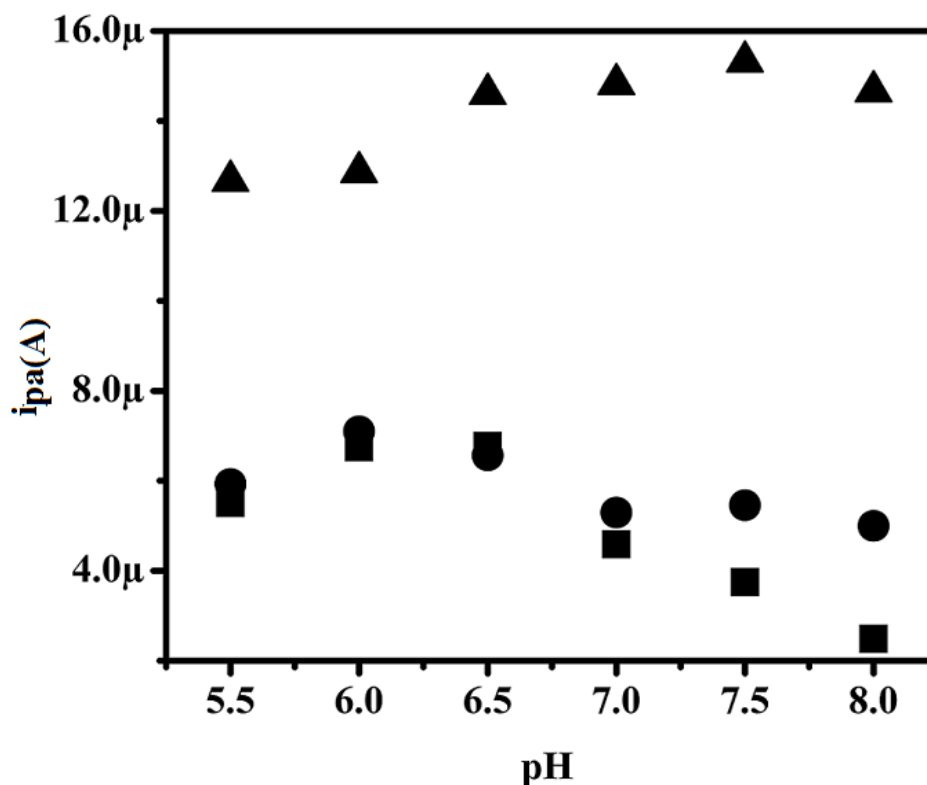


Figure 5. (▲) for a MCPE prepared with CTAB-NiO nanoparticles, (●) for a MCPE prepared with SDS-NiO nanoparticles and (■) for a bare CPE, the graph representation DA anodic peak current versus PBS pH 5.5 to 8.0 with a scanning rate of 0.1V/s.

The anodic peak current (i_{pa}) of DA increases at pH 7.5 PBS and the anodic peak current then decreases with further increases in the pH 8.0 PBS. The maximum anodic peak current occurred at pH 7.5 PBS. Therefore, PBS with a pH of 7.5 was chosen for all following electrochemical DA analyses and also anodic peak current response was enhanced in all pH PBS at the MCPEs prepared with CTAB-NiO nanoparticles as compared MCPE prepared with SDS-NiO nanoparticles and bare CPE.

3.4. Electrochemical response of DA at the bare electrode and the MCPE

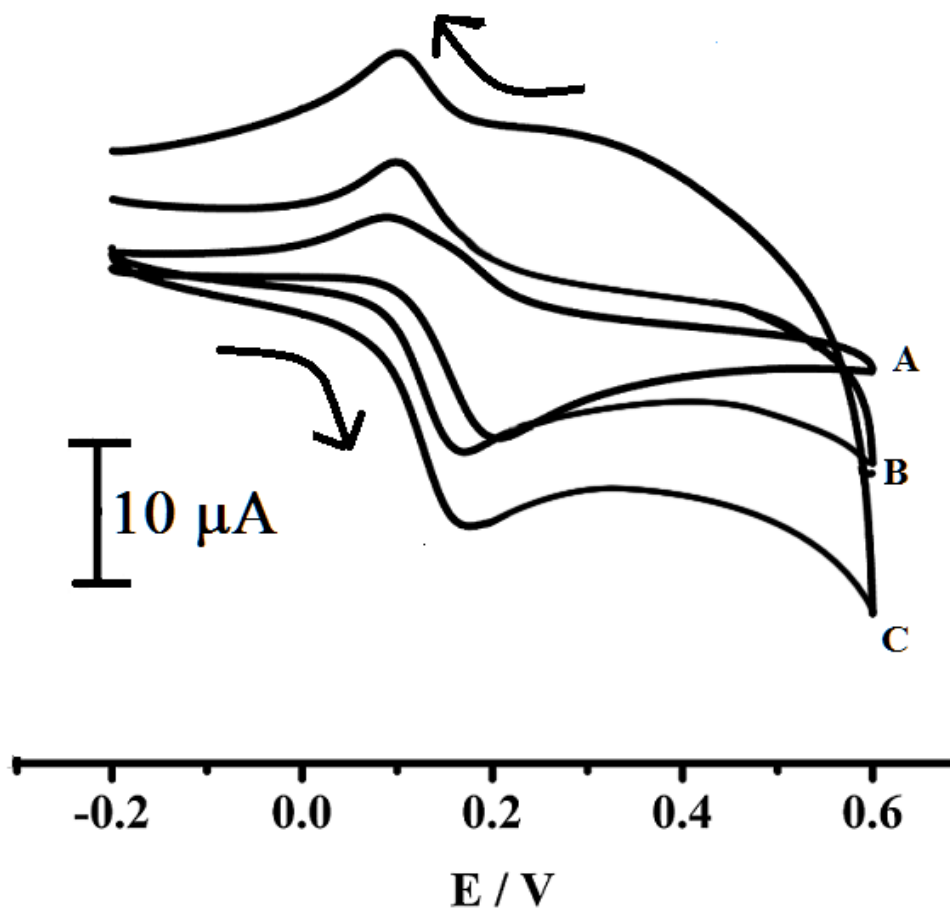


Figure 6. Cyclic voltammogram of 1×10^{-5} M DA in 0.2M PBS pH 7.4 at (A) bare CPE, (B) a MCPE prepared with SDS-NiO nanoparticles and (C) a MCPE prepared with CTAB- NiO nanoparticles.

The cyclic voltammograms responses of 1×10^{-5} M DA in 0.2 M PBS pH 7.4 at the bare CPE and at the MCPE prepared from SDS-NiO nanoparticles and CTAB-NiO nanoparticles were measured at a scan rate of 0.200 Vs^{-1} respectively are shown in Fig. 6(A)-(C). The result indicates both SDS-NiO nanoparticles and CTAB-NiO nanoparticles exhibit good electrochemical sensing and electrocatalytic activity than bare CPE and among MCPEs prepared from SDS-NiO nanoparticles and CTAB-NiO nanoparticles, the MCPEs prepared from CTAB- NiO nanoparticles exhibit enhanced redox peak current response than the MCPEs prepared from SDS- NiO nanoparticles. This may be due to NiO

nanoparticle form hydrogen bonds with the hydroxyl groups of DA, which would activate the hydroxyl groups and weaken the bond energy of OH⁻ to form dopaquinone [27], and also may be due to a small amount of CTAB surfactants present on the surface of NiO nanoparticles [19]. Therefore, MCPEs prepared from CTAB- NiO nanoparticles exhibit better sensing activity, and also used as an electrochemical sensor for detection of DA and also for detection of DA in the presence of AA, UA and BPA at physiological pH 7.4.

3.5. The effect of scan rate

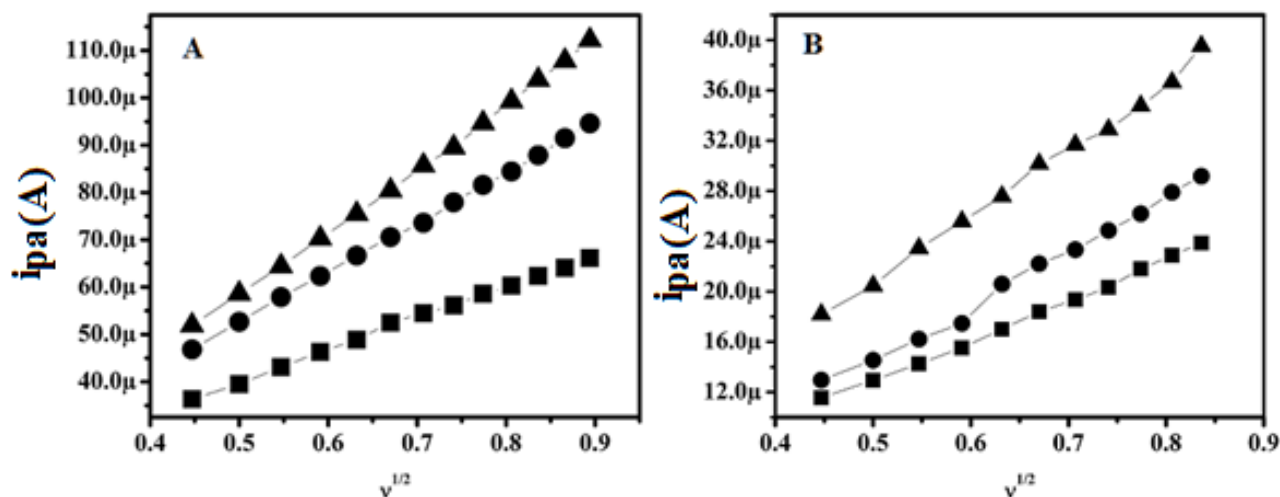


Figure 7. For MCPE prepared with SDS-NiO nanoparticles and CTAB-NiO nanoparticles with different scan rates (0.2, 0.25, 0.3, 0.35, 0.4, 0.45, 0.5, 0.55 and 0.6 V/s) in 0.2M PBS pH 7.4, the Fig. 7A shows graph of anodic peak current versus the square root of the scan rate for 1×10^{-3} M $K_4[Fe(CN)_6]$ for a MCPE prepared with CTAB-NiO nanoparticles (-▲-), for a MCPE prepared with SDS-NiO nanoparticles (-●-) and bare CPE (-■-) and Fig.7 B shows graphs of anodic peak current versus the square root of the scan rate for 1.0×10^{-5} mol/L DA for a MCPE prepared with CTAB- NiO nanoparticles (-▲-), for a MCPE prepared with SDS-NiO nanoparticles (-●-) and bare CPE (-■-).

The effect of scan rate for 1×10^{-3} M $K_4 [Fe(CN)_6]$ in 0.1M KCl and 1×10^{-5} M DA in 0.2 M PBS pH 7.4 was studied by CV at bare CPE, MCPEs prepared from SDS-NiO nanoparticles and CTAB-NiO nanoparticles. The graph obtained linearity between the square root of the scan rate ($v^{1/2}$) and anodic peak currents for bare CPE, the MCPE prepared with the SDS-NiO nanoparticles and CTAB-NiO nanoparticles are shown in Fig.7A (-■-, -▲- and -●- respectively) for $K_4 [Fe(CN)_6]$ and Fig.7B (-■-, -▲- and -●- respectively) for DA. The results of all the electrodes exhibited correlation coefficients of $r^2=0.998 \pm 0.001$. These results indicate that the electron-transfer reaction of bare CPE and MCPEs prepared with SDS-NiO nanoparticles and CTAB-NiO nanoparticles was a diffusion-controlled process.

3.6. The effect of the concentration of DA

The differential pulse voltammetry technique was used for analysis of DA concentration, which was varied from 1 to 800 μM . The results for the MCPEs prepared from CTAB-NiO nanoparticles are shown in Figs. 8 (A).

Table 1. Comparison of the analytical performances of different modified electrodes

| Electrode | Detection limit (μM) | Linear range (μM) | Techniques | References |
|----------------------------------|-----------------------------------|--------------------------------|------------|------------|
| LDH/CILE | 5.0 | 10-1100 | DPV | [29] |
| Au/Gr-Au | 30.0 | 10-100 | SW | [30] |
| Banana-MWCNTs MCPE | 2.09 | 10-30 | DPV | [31] |
| CTAB functionalized GO-MWCNT/GCE | 1.5 | 5-500 | DPV | [32] |
| Au-Gr/GCE | 1.86 | 1-1000 | DPV | [33] |
| Ag-reduced GO/GCE | 5.4 | 10-800 | LSV | [34] |
| CTAB-NiO nanoparticles /MCPE | 0.68 | 1-800 | DPV | This work |

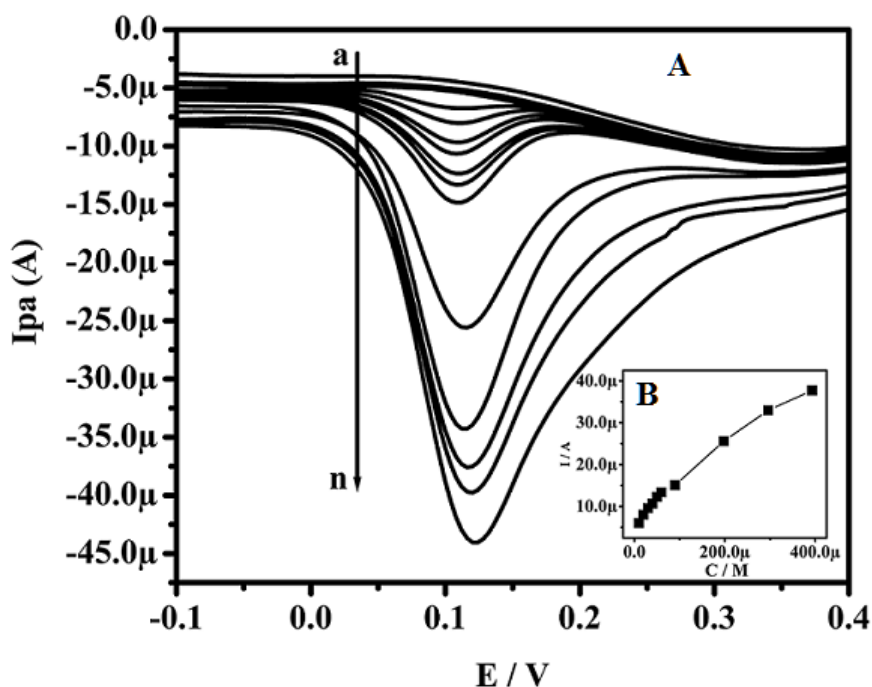


Figure 8A. Shows Differential pulse voltammogram of (a) 9.9×10^{-6} M, (b) 1.9×10^{-5} M, (c) 2.9×10^{-5} M, (d) 3.9×10^{-5} M, (e) 4.9×10^{-5} M, (f) 7.9×10^{-5} M, (g) 9.9×10^{-5} M, (h) 1.9×10^{-4} M, (i) 3.9×10^{-4} M, (j) 5.9×10^{-4} M and (k) 7.9×10^{-4} M DA in 0.2M PBS pH 7.4 at a MCPE prepared with CTAB- NiO nanoparticles and corresponding graph peak current versus concentration of DA shown in the inset Fig. 8B.

The corresponding graphs of anodic peak current versus concentration of DA shows two linear relationship ranges of 1 to 100 μM and 200 to 800 μM , with linear regression equations of $I_{pa} (\mu\text{A}) = 0.1438(C_{\mu\text{M}/L}) + 4.99 (\mu\text{A})$ and $I_{pa}(\mu\text{A}) = 9.545(C_{\mu\text{M}/L}) + 0.07494(\mu\text{A})$, respectively. The correlation coefficient for the first linearity was 0.995 and that for the second was 0.990 for the MCPE prepared with CTAB-NiO nanoparticles, as shown in Fig. 8 (B). The decrease in the sensitivity (slope) in the second linear range was due to kinetic limitations [28]. The detection limits for DA in the lower concentration range was $6.86 \times 10^{-7} \text{ M}$ for the MCPE prepared with CTAB-NiO nanoparticles. The MCPE prepared with CTAB-NiO nanoparticles demonstrated a relatively lower detection limit than compared with previous reported literatures [29,-34] (Table-1). From the table-1 it was shows that the MCPE prepared with CTAB-NiO nanoparticles exhibits low detection limit for detection of DA.

3.7. Electrochemical response for DA, AA, UA and BPA at MCPEs

Fig. 9A shows the electrochemical behavior of $1.5 \times 10^{-5} \text{ M}$ DA, $4.5 \times 10^{-5} \text{ M}$ UA, 2.5mM AA and $1.8 \times 10^{-5} \text{ M}$ BPA in 0.2 M PBS at pH 7.4 is MCPE prepared with CTAB- NiO nanoparticles and at the MCPE prepared with SDS/polyglycine/CTAB-NiO nanoparticles. The MCPE prepared with SDS/polyglycine/CTAB-NiO nanoparticles demonstrated an improved current response with sharp resolved peak for all analytes (DA at 0.21V, AA at - 0.011V, UA at 0.32V and BPA at 0.55V) is shown in solid line curve and dashed line curve shows overlapped single peak for all the analytes at a MCPE prepared with CTAB-NiO nanoparticles. This shows that MCPE prepared with SDS/polyglycine/CTAB- NiO nanoparticles exhibit good electrochemical determination of dopamine in presence of UA, AA and BPA at physiological pH.7.4.

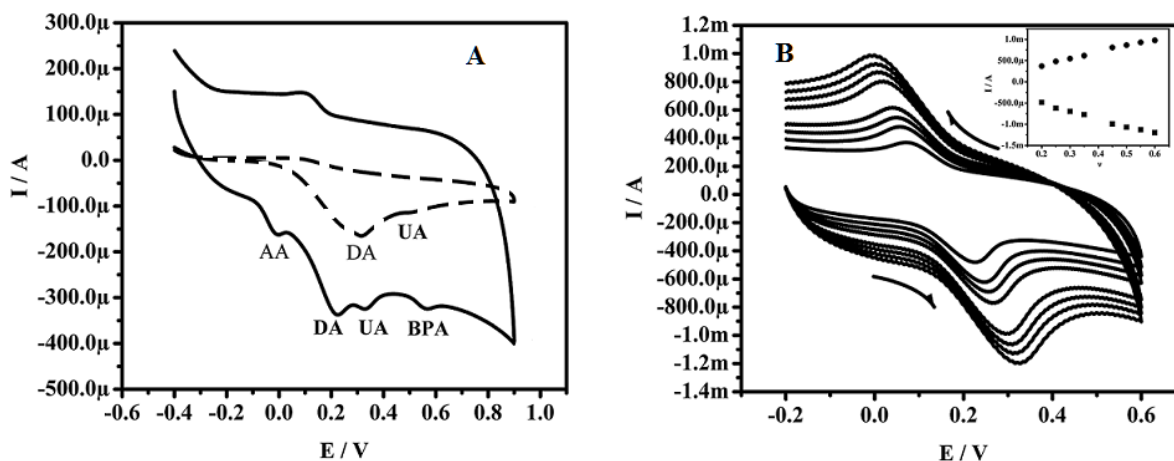


Figure 9A. shows Cyclic voltammograms of $1.5 \times 10^{-5} \text{ M}$ DA, $4.5 \times 10^{-5} \text{ M}$ UA, 2.5mM DA and $1.8 \times 10^{-5} \text{ BPA}$ in 0.2M PBS pH 7.4 at the a MCPE prepared with CTAB-NiO nanoparticles (curve shown in dashed line) and at the MCPE prepared with SDS/polyglycine/CTAB- NiO nanoparticles (curve shown in solid line) and Fig.9B shows Cyclic voltammograms of variation of scan rate for DA at SDS/ polyglycine/CTAB-NiO nanoparticles MCPE (0.2, 0.25, 0.3, 0.35, 0.4, 0.45, 0.5, 0.55 and 0.6 V/ s) in 0.2M PBS pH 7.4 and corresponding inset graph shows peak current versus scan rate of DA.

The Fig. 9B shows effect of the scan rate for DA was analyzed by CV at the MCPE prepared with SDS/polyglycine/CTAB-NiO nanoparticles; the results demonstrated an increase in the redox peak currents with an increase in the scan rate ($0.2\text{--}0.600\text{Vs}^{-1}$) and the graph obtained linearity between the scan rates versus redox peak current. The correlation coefficient was 0.9994, which indicates the electrode reaction process was adsorption-controlled [28, 35, 36].

Fig.10A shows differential pulse voltammograms of individual analytes oxidation peak potential for DA at 0.114V, AA at -0.083V, UA at 0.206V and BPA at 0.410V and also inserted differential pulse voltammogram shows simultaneous detection of DA, AA, UA and BPA in physiological pH 7.4 and Fig 10B shows electrochemical detection of DA in the presence of AA, UA and BPA is linearly increase anodic peak current with increase in concentration of DA and inserted graph shows linearity between anodic peak current and concentration of DA. Therefore, the MCPE prepared with SDS/polyglycine/CTAB-NiO nanoparticles was useful for selective detection of DA in the presence of AA, UA and BPA at physiological pH 7.4. The obtained results demonstrated the opportunity of a simultaneous multi-detection of bioactive molecules based on the DPV method.

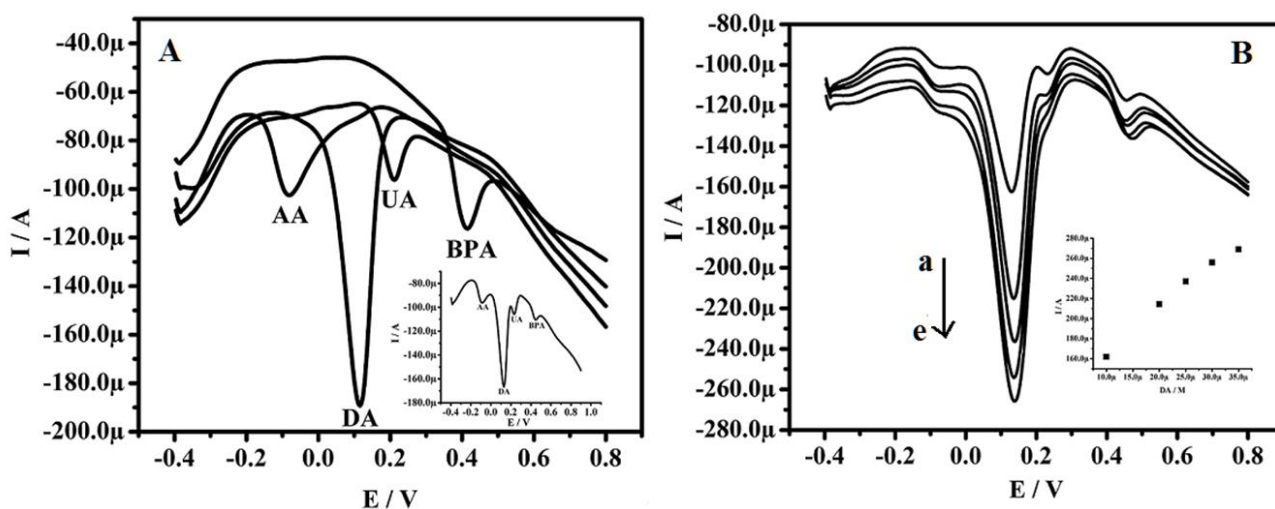


Figure 10. A shows Differential pulse voltammograms of individual $5 \times 10^{-4}\text{M}$ AA, $4 \times 10^{-4}\text{M}$ UA, $1.5 \times 10^{-4}\text{M}$ BPA and $2 \times 10^{-4}\text{M}$ DA in 0.2M PBS pH 7.4 at MCPE prepared with SDS/polyglycine/CTAB- NiO nanoparticles and corresponding Differential pulse voltammogram shows for all resolved oxidation peaks of AA, UA, BPA and DA. Fig. 10B shows Differential pulse voltammograms (a) $1 \times 10^{-5}\text{M}$, (b) $1.5 \times 10^{-5}\text{M}$, (c) $2.0 \times 10^{-5}\text{M}$, (d) $2.5 \times 10^{-5}\text{M}$, (e) $3.0 \times 10^{-5}\text{M}$ DA in 0.2M PBS pH 7.4 in the presence of $2.5 \times 10^{-3}\text{M}$ AA, $1.8 \times 10^{-5}\text{M}$ BPA, $4.5 \times 10^{-5}\text{M}$ UA at MCPE prepared with SDS/polyglycine/CTAB- NiO nanoparticles and corresponding graph shows anodic peak current versus concentration of DA in the presence of AA,UA and BPA

3.8. Application to real samples

The proposed MCPE prepared with SDS/polyglycine/CTAB- NiO nanoparticles was demonstrated by the quantitative detection of DA in human blood serum sample. The preparation

procedure followed is as follows; 10 mL of human serum sample without any treatment was diluted to 100 mL with pH 7.4 PBS. Different of volume this solution is mixed with the known volume concentration of known concentration DA solution in order to get different concentrations of spiked DA. Similarly drug injection capsule containing 200mg dopamine hydrochloride in 5ml of sterilized water (Sterile Specialities India Private Ltd.) is suitably diluted to get different known standard concentrations of DA and analyzed. Each experiment was carried out at least 5 times and the results are presented in Table. 2. The obtained recovery and relative standard deviation (RSD) seems to be good, indicating the better performance of the proposed method.

Table 2. Determination of DA in human blood serum and drug injection sample (number of trails =5).

| Samples | Spiked DA sample (μM) | Found (μM) | Recovery (%) | RSD (%) |
|----------------|------------------------------------|-------------------------|--------------|---------|
| Drug injection | 80 | 78.5 | 98.1 | 1.88 |
| | 160 | 156 | 97.5 | 1.15 |
| | 240 | 234 | 97.5 | 2.45 |
| Blood serum | 80 | 78.2 | 97.75 | 1.39 |
| | 160 | 155.5 | 97.1 | 0.99 |
| | 240 | 236 | 98.3 | 2.21 |

4. CONCLUSIONS

The NiO nanoparticles were synthesized using SDS and CTAB surfactants by co-precipitation method and the other electrochemical parameters are studied. The MCPE prepared from SDS/Polyglycine/CTAB-NiO nanoparticles shows effective electrochemical sensor towards electrochemical detection of DA in presence of AA, UA and BPA. The MCPE prepared from CTAB-NiO nanoparticles exhibits low detection limit for DA. The MCPE prepared from SDS/Polyglycine/CTAB-NiO nanoparticles demonstrated significant effect on peak currents for detection of dopamine with good electrochemical signal separation peak potential between for all the analytes (UA, AA and BPA). The proposed method was demonstrated good recovery for DA analysis in clinical and pharmaceutical sample. Therefore, the present method could be extended to many metal oxide for the synthesis of metal oxide modified electrodes with good electrocatalytic activities for the simultaneous investigation of DA, AA, UA, BPA and for bioactive molecules or neurotransmitters.

References

1. H. Sato, T. Minami, S. Takata and T. Yamada, *Thin Solid Films*. 236 (1993) 27.
2. A. Aslani, V. Oroojpour and M. Fallahi, *Appl. Surf. Sci.* 257 (2011) 4056.
3. B. Liu, H. Yang, H. Zhao, L. An, L. Zhang, R. Shi, L. Wang, L. Bao and Y. Chen, *Sens. Actuators, B*. 156 (2011) 251.
4. A. Salimi, E. Sharifi, A. Noorbakhsh and S. Soltanian, *Biophys. Chem.* 125 (2007) 540.

5. B. Moghaddam, M. R. Ganjali, R. Dinarvand, T. Razavi, A. A. Saboury, A. A. Moosavi-Movahedi and P. Norouzi, *J. Electroanal. Chem.* 614 (2008) 83.
6. S. Y. Chee, M. Flegel and M. Pumera, *Electrochem. Commun.* 13 (2011) 963.
7. A. Noorbakhsh and A. Salimi, *Biosens. Bioelectron.* 30 (2011) 188.
8. Y. Ding, Y. Liu, L. Zhang, Y. Wang, M. Bellagamba, J. Parisi, C. M. Li and Y. Lei, *Electrochim. Acta.* 58 (2011) 209.
9. A. Salimi, A. Noorbakhsh, E. Sharifi and A. Semnani, *Biosens. Bioelectron.* 24 (2008) 792.
10. S. Rezaei-Zarchi, S. Imani, A. Javid, A. M. Zand, M. Saadati and Z. Zagari, *Afr. J. Biochem. Res.* 5 (2011) 165.
11. A. S. Adekunle and K. I. Ozoemena, *J. Electroanal. Chem.* 645 (2010) 41.
12. L. Liu, Y. Zhang, G. Wang, S. Li, L. Wang, Y. Han, X. Jiang and A. Wei, *Sens. Actuators, B.* 160 (2011) 448.
13. K. Arora, M. Tomar and V. Gupta, *Biosens. Bioelectron.* 30 (2011) 333.
14. F. Xu, M. Gao, L. Wang, G. Shi, W. Zhang, L. Jin and J. Jin, *Talanta*, 55 (2001) 329.
15. H. F. Cui, Y. H. Cui, Y. L. Sun, K. Zhang and W. D. Zhang, *Nanotechnology*, 21 (2010) 215601.
16. E. Hirsch, A. M. Graybiel and Y. A. Agid, *Nature*, 334 (1988) 345.
17. R. M. Wightman, L. J. May and A. C. Michael, *Anal. Chem.*, 60 (1988) 769A.
18. J. W. Mo and B. Ogorevc, *Anal. Chem.*, 73 (2001) 1196.
19. S. Reddy, B. E. Kumara Swamy, and H. Jayadevappa, *Electrochim. Acta* 61 (2012) 78.
20. S. Reddy, B. E. K. Swamy, H. N. Vasana and H. Jayadevappa, *Anal. Methods*, 4 (2012) 2778.
21. S. Reddy, B. E. K. Swamy, M. Schell and H. Jayadevappa, *Chemical Sensors*, 4 (2014) 20.
22. V. V. S. E. Duttam and H. A. Mottola, *Anal. Chem.* 46 (1974) 1777.
23. C. A. Richter, L. S. Birnbaum, F. Farabollini, R. R. Newbold, B. S. Rubin, C. E. Talsness, J. G. Vandenberg, D. R. Walser-Kuntz and F. S. Vom Saal, *Reprod. Toxicol.* 24 (2007) 199.
24. N. B. Jonathan, E. R. Hugo and T. D. Brandebourg, *Mol Cell Endocrinol.* 304 (2009) 49.
25. J. H. He, S. L. Yuan, Z. M. Tian, Y. S. Yin, P. Li, Y. Q. Wang, K. L. Liu, S. J. Yuan, X. L. Wang and L. Liu, *Magn Magn Mater.* 320 (2008) 3293.
26. S. Reddy, B. E. Kumara Swamy, U. Chandra, B. S. Sherigara and H. Jayadevappa, *Int. J. Electrochem. Sci.* 5 (2010) 10.
27. G. Wang, J. Sun, W. Zhang, S. Jiao, B. Fang, *Mikrochim. Acta* 164 (2009) 357.
28. M. Mazloum-Ardakani, H. Rajabi, H. Beitollahi, B. B. Fatemah Mirjalili, A. Akbari and N. Taghavinia, *Int. J. Electrochem. Sci.* 5 (2010) 147.
29. Z. Zhu, L. Qu, Y. Guo, Y. Zeng, W. Sun and X. Huang, *Sens. Actuators, B.* 151 (2010) 146.
30. S. Pruneanu, A. R. Biris, F. Pogacean, C. Socaci, M. Coros, M. C. Rosu, F. Watanabe, A. S. Biris, *Electrochimica Acta* 154 (2015) 197.
31. J. B. Raoof, A. Kiani, R. Ojani, R. Valiollahi, *Anal. Bioanal. Electrochem.*, 3 (2011) 59-66.
32. Y. J. Yang, W. Li, *Biosens. Bioelectron.* 56 (2014) 300.
33. J. Li, J. Yang, Z. Yang, Y. Li, S. Yu, Q. Xu, X. Hu, *Anal. Methods* 4 (2012) 1725.
34. B. Kaur, T. Paniyan, B. Satpati, R. Srivastava, *Colloid. Surface. B.* 111 (2013) 97.
35. A. J. Bard, L. R. Faulkner, *electrochemical methods: Fundamental and Application*, Wiley, New York, 2000.
36. S. Corona-Avendano, G. Alarcon-Angles, M. T. Ramirez-Silva, G. Rosquete-pina, M. Ramero-Romo and M. Palomar-Pardave, *J. Electroanal. Chem.* 609 (2007) 17-26.